Nuclear Inst. and Methods in Physics Research B 465 (2020) 67–72

Contents lists available at ScienceDirect

Nuclear Inst. and Methods in Physics Research B

journal homepage: www.elsevier.com/locate/nimb

Photonuclear reactions by relativistic electron channeling radiation

O.V. Bogdanov[a,b,*], S.B. Dabagov[c,d,e], Yu.L. Pivovarov[a]

[a] National Research Tomsk Polytechnic University, Tomsk, Russia
[b] National Research Tomsk State University, Tomsk, Russia
[c] INFN laboratori Nazionali di Frascati, Frascati (RM), Italy
[d] RAS PN Lebedev Physical Institute, Moscow, Russia
[e] NR Nuclear University MEPhI, Moscow, Russia

ARTICLE INFO

Keywords:
Relativistic electrons
Channeling radiation
Nuclear photonics
Neutron source

ABSTRACT

The research for newly developing branch of nuclear physics, the nuclear photonics, has been accompanied since the beginning with the studies on intense MeV photon sources. One of the possible solution is in the use of channeling radiation. The channeling radiation spectrum for sub-GeV–several GeV electrons is characterized by a sharp maximum at photon energies up to several MeV, which is enough to excite separate nuclear levels as well as (γ,n) reaction for light Be and D nuclei. This maximum may even reach the region of giant dipole resonance for heavier nuclei. At equal radiator thickness the channeling radiation flux may exceed in more than one order that of bremsstrahlung. Thus, channeling radiation can be efficiently utilized in studying photonuclear reactions as well as generating pulsed neutron beams at sub-GeV electron accelerators. The latter is illustrated by detailed calculations of the neutrons yield from the light D and Be targets irradiated by channeling radiation. The non-trivial dependence of neutrons yield on the energy of incident electron beam and on the electron beam alignment with respect to the crystal channeling planes is revealed.

1. Photonuclear reaction studies at electron accelerators

The development of new methods to generate intense monochromatic MeV photon beams for precise studies of photo-nuclear reactions is the novel trend in nuclear physics (see e.g. in recent Conferences on Nuclear Photonics [1,2]). Besides photonuclear physics, there are important applications of photonuclear reactions mainly based on both generation and use of pulsed neutron beams in medicine, detection systems, etc.

"Old" method for studies of photonuclear reactions is related to the use of bremsstrahlung (BS), while BS is also widely used for generation of pulsed neutron beams [3–8]. The novel techniques to obtain the qualitative MeV-photon beams using FEL (e.g. at ELI, Romania) are only in progress [1,2].

Additionally to BS, other types of electromagnetic radiation can provide researchers with MeV photon beams. If based on the use of electron accelerators, they are mostly known as hard synchrotron radiation (SR) and channeling radiation (CR). The use of SR instead of BS was already suggested in [9] (SR-n processes). Similar to [9] in [10] it was suggested to utilize CR for photonuclear reaction studies (CR-n processes). However, for today only some qualitative estimates were given in [9,10]. Probably it is the reason that up to date, no experimental studies for SR-n processes are known. Moreover, the synchrotrons are typically large and expensive machines compared to modern linear electron accelerators (e.g. serving as injectors to the synchrotrons and storage rings).

On the contrary to the SR-n process, the CR-n one was studied in two earlier experiments [11,12]. The measurements of photoneutrons yield produced by CR in several light and heavy targets ($H_2{}^1O$, $H_2{}^2O$, H^2, Be, Bi) where CR was emitted by 900 MeV channeled electrons in a 0.35 mm thick ⟨1 1 0⟩ diamond crystal, have revealed remarkable dependence of the photoneutrons yield on the tilting angle of the diamond crystal with respect to the electron beam. In the experiments at fixed electron beam energy (900 MeV) the orientation effect was observed.

In this paper we present the results of our investigations on another specific phenomenon for the CR-n process. As known, the CR spectrum from sub-GeV or several GeV electrons is characterized by well pronounced maximum at photon energies from 100 keV up to 5 MeV [13,14], while its intensity may essentially (1–2 orders of magnitude) exceed the BS intensity at equal targets' thickness. The position of this maximum is strongly defined by the electron beam energy, tuning of which may lead to the coincidence of CR and (γ, n) reaction maxima. Thus, CR photons may efficiently excite different photonuclear

* Corresponding author at: National Research Tomsk Polytechnic University, Tomsk, Russia.
E-mail address: bov@tpu.ru (O.V. Bogdanov).

https://doi.org/10.1016/j.nimb.2020.01.005
Received 21 May 2019; Received in revised form 29 December 2019; Accepted 9 January 2020

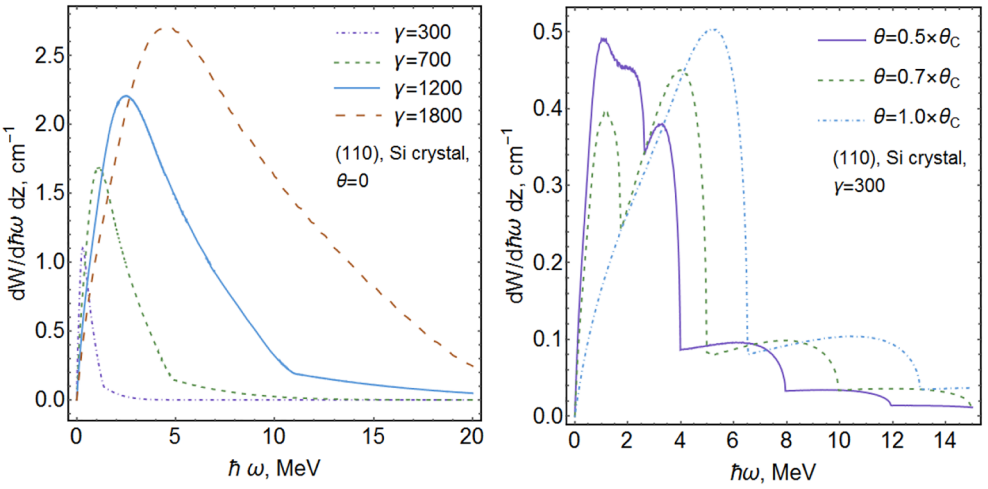

Fig. 1. Spectral distributions of the CR intensity for relativistic electrons channeled in (1 1 0) Si crystal calculated according Eq. (1): a) (left panel) for a number of fixed relativistic factors at zero incidence angle with respect to (1 1 0) Si planes; b) (right panel) for different incident angles with respect to (1 1 0) Si planes at relativistic factor $\gamma = 300$. Here, θ_C is the critical angle for channeling and θ stands for the angle of incidence.

reactions in the downstream production target.

In this work we consider (γ, n) reactions on light nuclei (D and Be) induced by CR. We have analyzed dependences of the reactons yield on both electron beam energy and beam-crystal alignment. Some advantages of the CR use with respect to the BS use are underlined.

2. Channeling radiation spectra

The CR spectrum by sub-GeV or GeV electrons [13,14] is rather complicated function of photon energy. In order to calculate the CR spectra we have performed computer simulations based on earlier developed BCM-1.0 code [15,16]. This code allows numerical calculation of relativistic channeled electron trajectory and corresponding CR spectrum using the well-known formulae of classical electrodynamics. The trajectory and corresponding CR spectrum depend on initial conditions: point of incidence and angle of incidence with respect to the channeling planes. The averaging over simulated trajectories is included into the BCM-1.0 code.

As expected our simulations have shown that the CR photon intensity strongly depends on the initial electron beam energy as well as on the angle of beam momentum with respect to crystallographic planes or axes. For simplicity we consider the planar channeling of sub-GeV–GeV electrons in a crystal. For the known electron trajectory defined in our case by computer simulations, the expression for CR intensity per one electron and unit crystal length reads [13]:

$$\frac{dW}{d\omega\, dz} = \frac{e^2\omega}{c^4T^2}\sum_{n=1}^{\infty}\Theta\left(1-\frac{\omega T}{4\pi n\gamma^2}\right)\left(1-\frac{T\omega}{2\pi\gamma^2 n}+\frac{1}{2}\left(\frac{T\omega}{2\pi\gamma^2 n}\right)^2\right)|v_{\tilde{\omega}}^T|^2, \tag{1}$$

$$v_{\tilde{\omega}}^T = \int_0^T v_\perp(t)e^{i\tilde{\omega}t}dt,\ \tilde{\omega} = \frac{2\pi n}{T}.$$

here $\Theta(1-\omega T/4\pi n\gamma^2)$ is the Theta-function, T is the electron oscillation period in a planar channel, $v_{\tilde{\omega}}^T$ is the Fourier component of transverse electron velocity; γ is the electron relativistic factor, and $\hbar\omega$ is the photon energy. Further averaging of Eq. (1) over different electron trajectories allows getting the CR intensity by the electron beam crossing the crystal.

We suggest here that the electron oscillation period T in a planar channel remains constant for a simulated electron trajectory. In reality, T changes during the electron motion through a crystal due to multiple scattering (MS). Qualitatively, we may say that MS increases the transverse energy of channeled electron, thus increases T and softens the CR spectrum. When the transverse energy of channeled electron in the planar channeling potential becomes positive, the dechanneling occurs and an electron moves periodically intersecting the crystal planes, the T value decreases up to 2 times and the CR spectrum becomes again more hard [13]. In our consideration we neglect the multiple scattering (MS), which destroyers the defined (simulated) periodic and quasi-periodic channeling trajectories with increasing of penetration length L. The estimation on how MS could affect the sub-GeV and GeV electrons channeling and CR was the subject of numerous studies, see e.g. for earlier references in [13,14] and more recent papers [17–27]. This process is called dechanneling and characterized by dechanneling length L_d. Roughly speaking, L_d is the penetration length, at which the MS angle becomes equal to the Lindhard critical channeling length. The recent results [17,18] on MS studies for sub-GeV and GeV electrons channeling in (1 1 0) Si crystal showed that the dechanneling length varies within 15 – 50 μm. The dechanneling changes the channeling radiation spectra in the thick ($L > L_d$) straight and bent crystals, see in [17–27], thus can influence the CR-n process. In our work we considered the thin crystal target as the source of CR for photonuclear experiments instead of conventional thick bremsstrahlung target [3–8]. To conclude, the MS influence on CR is interesting problem, but here we restrict our consideration by thin crystal neglecting the change of T.

In the photonuclear physics experiments one deals usually with collimated BS. In order to take into account the collimation of a CR photon beam, we can modify Eq. (1) substituting the velocity term by one combined with the collimation factor

$$v_{\tilde{\omega}}^T \to \Theta\left(\frac{\omega T}{4\pi n\gamma^2}+\frac{\omega T}{4\pi n\gamma^2}\gamma^2\theta_{Coll}^2-1\right)v_{\tilde{\omega}}^T$$

where θ_{Coll} is the CR photon beam collimation angle. The collimation suppresses the CR soft part decreasing in such a way the radiation background.

The CR spectrum depends on the crystal type, the incidence angle for electrons with respect to the crystal planes that should not exceed several Lindhard angles (Lindhard angle θ_C is the critical angle for channeling), the crystal thickness, which should be less than the dechanneling length (for details, see in [13–14,17,18]).

Fig. 1a presents calculated CR spectral distributions for relativistic electrons in a (1 1 0) Si crystal at different fixed relativistic factors and at zero angle between the electron momentum and the (1 1 0) crystal planes. The results confirm that CR spectra become shifted to higher photon energies at the increase of the electron beam energy.

Fig. 1b shows the spectra for electrons with $\gamma = 300$ moving at various incident angles with respect to (1 1 0) Si planes. That means, at fixed γ the CR spectrum can be smoothly changed (fine tuning) manipulating the crystal orientation.

In general, at fixed electron energy, on the contrary to the ordinary BS in amorphous, the CR spectrum reveals strong dependence on the

electron beam orientation with respect to the direction of a crystal channeling plane. This feature can be utilized for handling the CR-n spectrum that is an advantage of crystal target compared to amorphous one. The physical reason is in transition from completely under-barrier (channeling) trajectories to above-barrier ones (quasi-channeling) that leads to shifting the peak in CR spectrum to higher energy (see in Fig. 1, right panel). In particular, this explained the disappearance of the peak around 1 MeV when the incidence angle is equal to θ_C.

3. Deuteron and Be photodisintegration cross-sections

The photonuclear cross-sections are rather complicated functions of the photon energy and usually are tabulated [28–31]. Among stable isotopes the lowest binding energies correspond to Be (1.665 MeV) and D (2.25 MeV) nuclei (see, e.g. [28–31]). In the case of photonuclear reaction D $\gamma \rightarrow$ n p the cross-section is defined by the sum of both electric and magnetic dipoles cross-sections and can be analytically described as follows [32]:

$$\sigma_{E_1} = \frac{8\pi\alpha}{3}\frac{\hbar^2c^2\sqrt{\varepsilon}}{Mc^2}\frac{(\omega-\varepsilon)^{3/2}}{\omega^3}\frac{1}{1-\gamma_t r_t}, \tag{2}$$

$$\sigma_{M_1} = \frac{2\pi\alpha}{3}\left(\frac{\hbar c}{Mc^2}\right)^2(\mu_p-\mu_n)^2\frac{\sqrt{\varepsilon}(\sqrt{\varepsilon}+\sqrt{\varepsilon_0})^2(\omega-\varepsilon)^{1/2}}{\omega(\omega+\varepsilon_0-\varepsilon)}\frac{1}{1-\gamma_t r_t} \tag{3}$$

here, α is the fine structure constant, $\gamma_t = \sqrt{M\varepsilon}/\hbar$, $r_t = 1.75 fm$ is the D triplet radius, $\varepsilon = 2.25 MeV$ is the D binding energy; $\varepsilon_0 = 0.067 MeV$ is the energy of a virtual singlet level, μ_p, μ_n are the magnetic moments of a proton and a neutron expressed in nuclear magnetons, Mc^2 and $\hbar\omega$ stand for the proton mass and the photon energy, respectively. Both magnetic and electric dipoles D photodisintegration cross-sections are shown in Fig. 2, demonstrating, respectively, well pronounced maxima near the photon energies 2.25–3 MeV and 4–6 MeV.

In the case of Be nuclei we do not have analytical expression for the cross-section of (γ, n) reaction and, thus, we have used its graphical representation and numerical values from [28–31] (see in Fig. 2, right panel).

4. CR-n process for D and Be targets

4.1. Dependence on electron beam energy

Let analyze the CR-n process based on the use of CR generated by channeled electrons with energies 300–1800 MeV (e.g., LNF facilities [33] and MAMI [34]) in a Si (1 1 0) crystal and successfully focused on a D or Be target. The neutron yield can be calculated as

$$Y(\gamma) = \int_{\varepsilon}^{\infty} d\hbar\omega \cdot N_{CR}(\gamma, \hbar\omega)\cdot[\sigma_{ph}(\hbar\omega)] \tag{4}$$

here $N_{CR}(\gamma, \hbar\omega)$ is the CR photon number, $\sigma_{ph}(\hbar\omega)$ is the (γ, n) reaction cross-section, and ε is the reaction threshold.

We start analysing how the key value, a convolution of the photodisintegration cross-section and CR photon flux depends on the energy of incident electrons. In the case of deuteron Eq. (4) can be presented in the form

$$Y(\gamma) = \int_{\varepsilon}^{\infty} d\hbar\omega \cdot N_{CR}(\gamma, \hbar\omega)\cdot[\sigma_{E1}(\hbar\omega) + \sigma_{M1}(\hbar\omega)] \tag{5}$$

The $Y(\gamma)$ value depends on relativistic factor γ of channeled primary electrons, which emit CR photons in a crystal. The photon number $N_{CR}(\gamma, \hbar\omega)$ of Eq. (4) is defined by the CR spectrum (2)

$$N_{CR}(\gamma, \hbar\omega) = \frac{1}{\hbar\omega}\cdot\frac{dW}{d\hbar\omega dz} \tag{6}$$

In order to understand better how the change in relativistic factor of incident electron beam may influence the neutron flux, a product of the CR photon number (6) and D photodisintegration cross-section (2), (3), for photon energies from D photodisintegration threshold ($E_{ph} > 2.25$ MeV) up to infinity, is presented in Fig. 3.

The product of the same CR photon number (6) and Be photodisintegration cross-section (Fig. 2, right part), for photon energies from Be photodisintegration threshold ($E_{ph} > 1.665$ MeV) up to infinity, is presented in Fig. 4.

The CR photon numbers used in plotting of Figs. 3 and 4 are simulated using Eq. (1) and Eq. (6) for the case of zero incident angle of electrons with respect to (1 1 0) Si planes.

Having calculated results similar to presented in Figs. 3 and 4 but for higher primary electron energies, the evaluation of an integral of Eq. (5) for D target and Eq. (4) for Be target is straightforward, and the results are presented in Fig. 5.

As follows, the change of channeled electrons relativistic factor results in very specific dependences of the CR-n reactions yield on that factor. As we can conclude from Fig. 4, a change in electron beam relativistic factor from $\gamma = 1000$ up to $\gamma = 5000$ results in specific behavior of CR-n reaction yield. The maximal increase is about 25 times in the case of D target and about 12 times in the case of Be target.

If the ordinary BS (the Bethe-Heitler-Shiff photon spectrum) is used instead of CR, the equal increase of the incident electron beam energy almost does not influence the B-n yield as seen from two lower curves in Fig. 5. It is explained by the fact that the increase of electron energy results in higher BS intensity for the hard tail of spectrum, while for D/

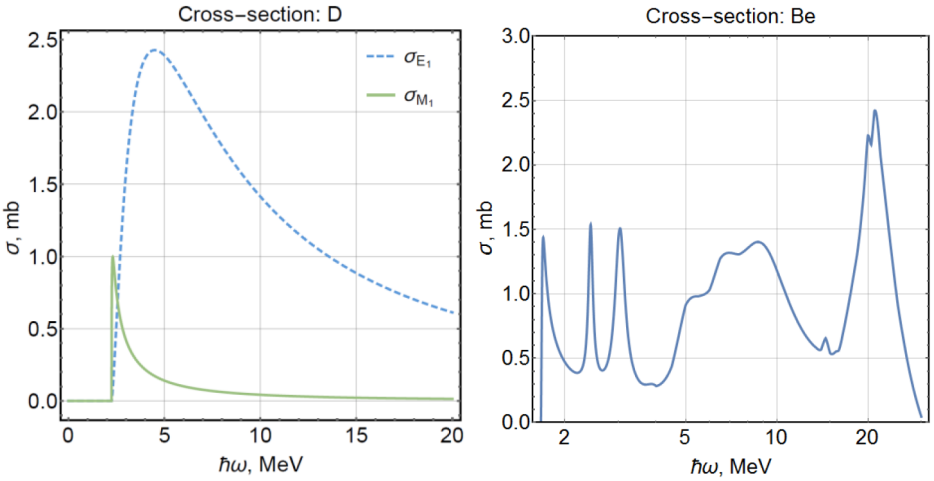

Fig. 2. Deuteron and Beryllium photodisintegration cross-sections as functions of photon energy. Left panel: Both electric and magnetic dipole contributions for D [32] shown separately. Right panel: The cross-section for the reaction (^{9}Be,γ) → (^{8}Be,n) [28–31].

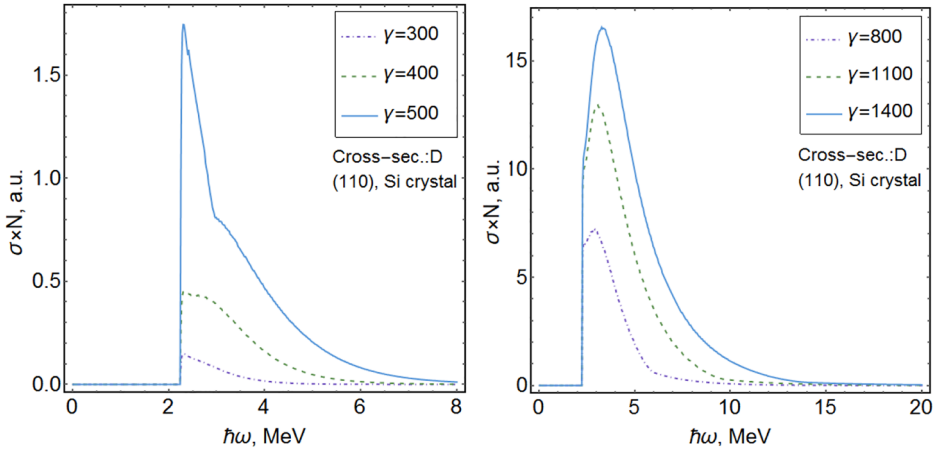

Fig. 3. The product of D photodisintegration cross-section and CR photon number for various electron relativistic factors (the integrand of Eq. (4)).

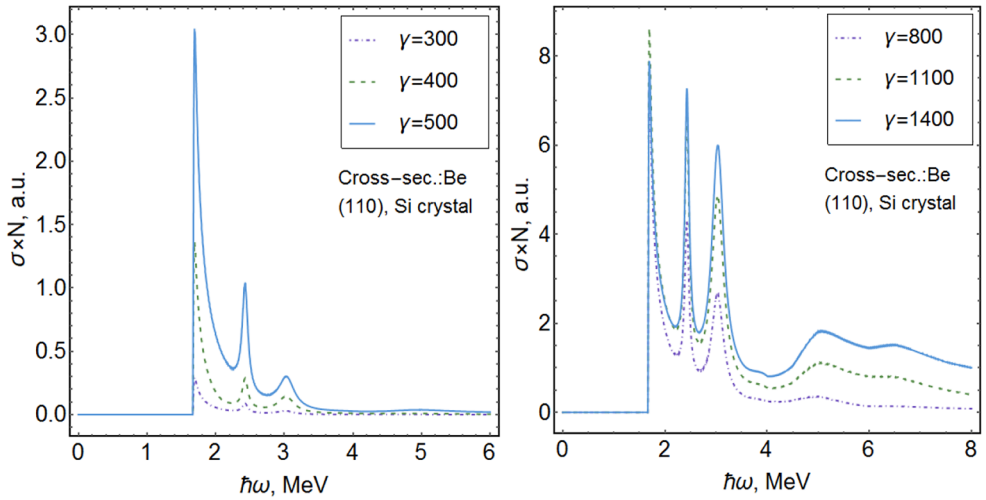

Fig. 4. The product of Be photodisintegration cross-section and CR photon number for various electron relativistic factors (the integrand of Eq. (4)).

Be photodisintegration reaction only the soft part of spectrum is affected. Successfully this part only slightly changes at the increase of the incident electron beam energy.

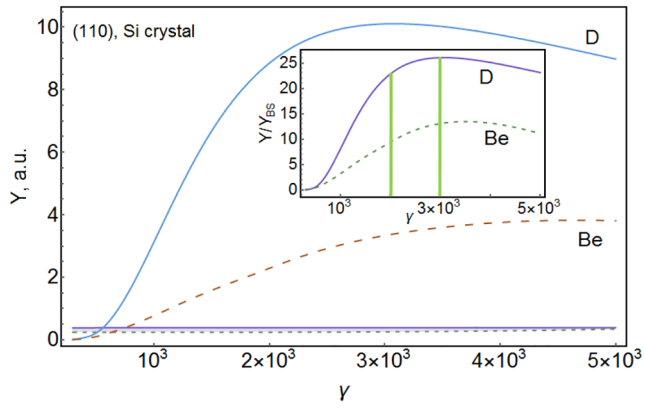

Fig. 5. Evaluated integrals of Eq. (4) for Be target and of Eq. (5) for D target, in arbitrary units, show the huge increase of the yield for the D and Be photodisintegration due to (γ, n) reaction by CR in dependence on electrons relativistic factor. The insert shows the ratio of CR-n yield to the BS-n yield (the same thickness of BS target). The vertical green lines are necessary in the Section 4.2. (For interpretation of the references to colour in this figure legend, the reader is referred to the web version of this article.)

At the fixed electron incident angle with respect to the crystal planes, on the contrary to the ordinary BS in amorphous target, the CR spectrum reveals strong dependence on the electron beam energy, see in Fig. 1a. It is not so in the case of well-known "standard" BS spectrum (Bethe-Heitler or Shiff spectrum) when its shape changes remarkably at its hard part. This specific dependence of CR spectrum on electron beam energy can be utilized for handling the CR-n process that is an advantage of crystal target compared to amorphous one.

4.2. Dependence on electron beam – Crystal alignment (orientation effect)

At fixed electron energy, on the contrary to the ordinary BS in amorphous, the CR spectrum reveals strong dependence on the electron beam orientation with respect to the direction of a crystal channeling plane. This feature can be utilized for handling the CR-n spectrum that is an advantage of crystal target compared to amorphous one. The physical reason is in transition from completely under-barrier (channeling) trajectories to above-barrier ones (quasi-channeling) that leads to shifting the peak in CR spectrum to higher energy (see in Fig. 1, right panel).

Fig. 6 shows the same ratios as presented in Fig. 5 (insert), but now for three different incident angles of electron beam with respect to (1 1 0) Si crystal planes, that are $\theta = 0.5\ \theta_C$ (solid line), $\theta = 0.7\ \theta_C$ (dotted line) and $\theta = 1.0\ \theta_C$ (dash-dotted line). The Fig. 5 (insert, $\theta = 0$) and Fig. 6 let make conclusion on existence of the prominent orientation effect.

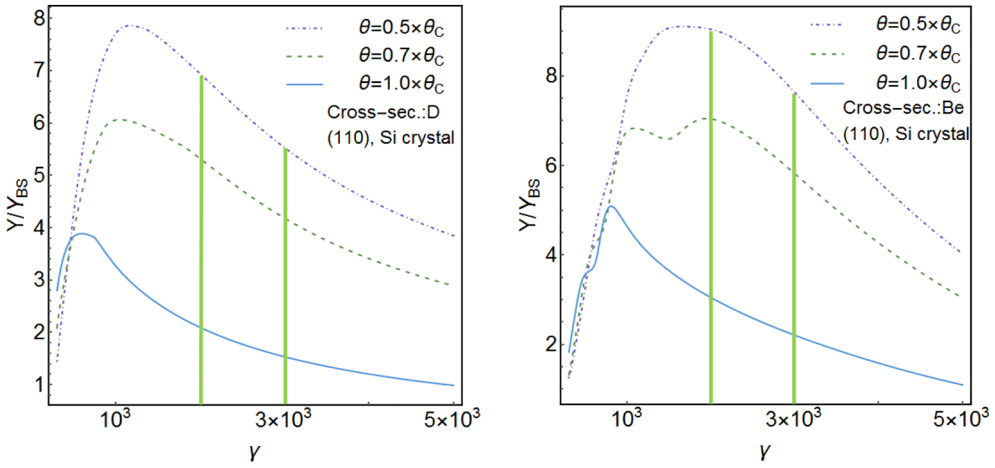

Fig. 6. The ratios of CR-n yield Y to BS-n yield Y_B for D target (left panel) and for Be target (right panel) for three values of incident angles of electron beam with respect to (1 1 0) Si crystal planes plotted as a function of electrons relativistic factor. The presence of green vertical lines is discussed in the text. (For interpretation of the references to colour in this figure legend, the reader is referred to the web version of this article.)

The remarkable change of the yield of (γ, n) reaction on D target by CR in dependence on electron beam alignment and at fixed relativistic factor is clearly seen. For example, at $\gamma = 2 \times 10^3$ the ratio drops from about 20.6 to 2.5 for D based reaction (intersections of green vertical lines with the curves in Fig. 4 (insert) and Fig. 5) following an increase in incident angle θ from zero to the critical channeling angle θ_C. Moreover, at $\gamma = 3 \times 10^3$ this ratio drops even more prominent, from about 25 ($\theta = 0$) up to 1.6 ($\theta = \theta_C$). In the case of Be target this ratio drops not so drastically, from about 10 ($\theta = 0$) to about 3 at $\gamma = 2 \times 10^3$ and from about 10 ($\theta = 0$) to about 2.3 ($\theta = \theta_C$) at $\gamma = 3 \times 10^3$.

The results of both Figs. 5 and 6 prove the orientational effect for CR-n as a fine tuning procedure allowing definition of the photonuclear cross-section. It is much more powerful instrument compared to large-scale tuning procedure based on manipulation of the electron beam energy.

4.3. CR photon beam collimation influence

Now let discuss the collimation influence for a CR photon beam and its influence on CR-n process. To simulate the CR photon numbers taking account of collimation, now is necessary to use modified Eq. (1), as discussed in Section 1. The simulation results are presented in Fig. 7.

The collimation is additional to relativistic factor γ parameter which defines the number of CR photons with energies necessary for (γ, n) reaction (approximately 2.25 – 20 MeV for D and 1.65 – 25 MeV for Be). It decreases the CR-n yield Y, (a.u.), while it maximum becomes more brilliant (see in Figs. 5 and 7).

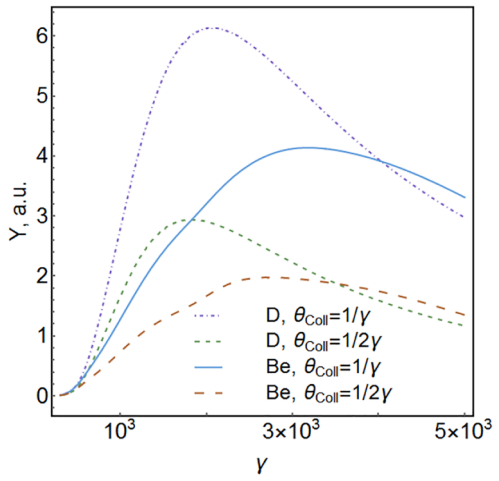

Fig. 7. The same as in Fig. 5, but taking into account the CR photon beam collimation: $\theta_{Coll} = 1/\gamma$ and $\theta_{Coll} = 1/2\gamma$.

Obviously, we have presented here just preliminary studies based on theoretical model and simulations. The unusual non-linear dependence of CR-n yield on electron beam energy and orientation effect could be the subject of future experimental studies.

5. Conclusions

To summarize, our analysis has shown that application of CR instead of BS for equal thickness targets to study photonuclear reactions reveals important advantages as follows.

First, there appears a large scale effect: a change in electron beam relativistic factor from $\gamma = 1000$ up to $\gamma = 5000$ results in specific enhancement of CR-n reaction yield. For instance, the increase of electron beam energy from 500 MeV up to 3000 MeV leads to about 25-fold (D target) and 12-fold (Be target) photonuclear reaction yield enhancement in the case of CR compared to that initiated by BS.

Second, there arises additional fine tuning effect: a possibility to change slightly the photonuclear reaction yield at fixed electron energy combined with the orientation effect for CR spectrum tuning.

Planar channeling radiation in a Si crystal has been analyzed, while in the case of axial channeling in more heavy crystal the predicted above features of CR-n reaction can be even more promising for applications. Indeed, the axial channeling potential is deeper than the planar one, that means both the critical channeling angle θ_C and the dechanneling length are greater. It is important from the point of view of simpler crystal alignment with account of initial electron beam angular spread and simpler manufacture of the thin crystals ($L < L_d$) for hybrid (combined) CR-n target. The important is that the axial CR spectrum is more intensive compared to planar CR ones, but simultaneously is much broader [13,14], that means the part of CR photons is beyond the regions of (gamma, n) cross-sections for D and Be. We restricted here our consideration by planar channeling CR for the sake of simplicity and since the simulations of CR at axial channeling takes much more computer time and should be a subject of separate paper.

As the photon number of CR photons may exceed in more than one order that of bremsstrahlung (BS) for equal radiator thickness, this might be an advantage for the CR utilization instead of traditional BS in studying photonuclear reactions as well as generating pulsed neutron beams at sub-GeV electron accelerators.

CRediT authorship contribution statement

O.V. Bogdanov: Visualization, Investigation, Software, Writing - original draft. **S.B. Dabagov:** Data curation, Writing - review & editing. **Yu.L. Pivovarov:** Supervision, Writing - review & editing.

Declaration of Competing Interest

The authors declare that they have no known competing financial interests or personal relationships that could have appeared to influence the work reported in this paper.

Acknowledgements

We are thankful to H. Backe, W. Lauth and for fruitful conversations.

This research was supported by the Tomsk Polytechnic University Competitiveness Enhancement Program grant and by the Tomsk State University competitiveness improvement programme. One of the authors (SD) would like to acknowledge the support by the Competitiveness Program of NRNU MEPhI (Moscow).

Appendix A. Supplementary data

Supplementary data to this article can be found online at https://doi.org/10.1016/j.nimb.2020.01.005.

References

[1] 1st International Conference on Nuclear Photonics, June 24-29, 2016, California, USA. Abstract Book: http://nuclearphotonics2016.ca.
[2] 2nd International Conference on Nuclear Photonics, June 24-29, 2018, Brasov, Romania. Abstracts Book: http://nuclearphotonics2018.eli-np.ro.
[3] V.G. Nedorezov, A.B. Savel'ev-Trofimov, Phys. At. Nucl. 80 (9) (2017) 1477–1483.
[4] V.P. Kovalev, Secondary emissions at electron accelerators. Moscow, Atomizdat, 1979, in Russian.
[5] J.L. Jones, et al., Nucl. Instrum. Meth. B 261 (2007) 326–330.
[6] S. Janek, et al., Phys. Med. Biol. 51 (2006) 5769.
[7] T. Gozani, M.J. King, Nucl. Instrum. Meth. A 805 (2016) 101–115.
[8] J. Stevenson, et al., Nucl. Instrum. Meth. A 652 (2011) 124–128.
[9] I.P. Eremeev, JETP Lett. 27 (1) (1978) 10–14.
[10] I.P. Eremeev, M.A. Kumakhov, Phys. Lett. A 72 (1979) 359–360.
[11] V.M. Golovkov, et al., Nucl. Instrum. Meth. 212 (1–3) (1983) 167–172.
[12] Yu.N. Adishchev, et al., JETP Lett. 33 (9) (1981) 478.
[13] V.N. Baier, V.M. Katkov, V.M. Strakhovenko, Electromagnetic Processes at High Energies in Oriented Single Crystals, World Scientific, Singapore, 1998.
[14] A.V. Korol, A.V. Solovev, W. Greiner, Channeling and Radiation in Periodically Bent Crystals. Springer Series on Atomic, Optical, and Plasma Physics, Springer-Verlag, Berlin-Heidelberg, 2013, , https://doi.org/10.1007/978-3-642-31895.
[15] O.V. Bogdanov, K.B. Korotchenko, Yu.L. Pivovarov, T.A. Tukhfatullin, Nucl. Instrum. Meth. B 266 (2008) 3858–4386.
[16] S.V. Abdrashitov, O.V. Bogdanov, S.B. Dabagov, Y.L. Pivovarov, T.A. Tukhfatullin, Nucl. Instrum. Meth. B 309 (2013) 59–62.
[17] H. Backe, W. Lauth, T.N.T. Thi, Nucl. Instrum. Meth. B 355 (2015) 24–29.
[18] H. Backe, W. Lauth, T.N.T. Thi, J. Instrum. 13 (4) (2018) C04022.
[19] O.V. Bogdanov, S.B. Dabagov, J. Phys. Conf. Ser. 357 (2012) 012029.
[20] H. Salehi, B. Azadegan, S. Shafeei, M. Nucl. Instrum. Meth. B 433 (2018) 43–50.
[21] B. Azadegan, W. Wagner, A.A. Savchenko, A.A. Tishchenko, Radiat. Phys. Chem. 157 (2019) 84–90.
[22] H. Backe, P. Kunz, W. Lauth, A. Rueda, Nucl. Instrum. Meth. B 266 (2008) 3835.
[23] L. Bandiera, et al., Phys. Rev. Lett. 115 (2015) 025504.
[24] A. Mazzolari, et al., Phys. Rev. Lett. 112 (2014) 135503.
[25] A. Sytov, et al., Eur. Phys. J. C 77 (2017) 901.
[26] S.B. Dabagov, N.K. Zhevago, La Rivista del Nuovo Cimento – 2008. – V.31 (9) pp. 491–529.
[27] O.V. Bogdanov, K.B. Korotchenko, Yu.L. Pivovarov, J. Phys. B. 41 (2008) 055004–P.1-8.
[28] Center for Photonuclear Experiments Data (Lomonosov Moscow State University, Skobeltsyn Institute for Nuclear Physics): http://cdfe.sinp.msu.ru/ind.
[29] National Nuclear Data Center: http://www.nndc.bnl.gov.
[30] B.L. Berman, Atlas of photoneutron cross sections obtained with monoenergetic photons, At. Data Nucl. Data Tables (1973).
[31] S.S. Dietrich, B.L. Berman, Atlas of photoneutron cross sections obtained with monoenergetic photons, At. Data Nucl. Data Tables 38 (1988) 99.
[32] G.E. Brown, A.D. Jackson, Nucleon-Nucleon Interaction, North-Holland Publishing Company, 1975.
[33] Laboratori Nazionali di Frascati: http://w3.lnf.infn.it/accelerators/.
[34] Johannes Gutenberg University Mainz: https://research.uni-mainz.de/.